10

Surface preparation of SS316L(N)-IG second mirrors for ITER optical diagnostics

© I.B. Tereschenko[1], D.S. Samsonov[1], E.E. Mukhin[1], G.V. Marinin[2], D.V. Terentev[2], V.E. Patrikeev[3], A.L. Khudoley[4], P.N. Kumeisha[4], V.D. Kalganov[5], K.A. Benken[6]

[1] Ioffe Institute,
St. Petersburg, Russia
[2] Russian Technologies,,
St. Petersburg, Russia
[3] JSC Lytkarino Optical Glass Plant (LZOS),
Lytkarino, Russia
[4] A.V. LYKOV INSTITUTE OF HEAT AND MASS TRANSFER (ITMO),
Minsk, Belarus
[5] Interdisciplinary Resource Centre for „Nanotechnology“
SPbU, St. Petersburg, Russia
[6] The Centre for Microscopy and Microanalysis (CMM) of SPbU ,
St. Petersburg, Russia

e-mail: i.tereschenko@mail.ioffe.ru

Received May 13, 2025
Revised July 24, 2025
Accepted August 04, 2025

The challenges of developing large-scale 316L(N)-IG mirrors for the collection system of the ITER divertor Thomson scattering (DTS) diagnostic are under consideration. These are second mirrors (M2), located out of direct plasma sight, require an optically smooth surface to ensure efficient light collection. Two approaches to surface finishing abrasive and magnetorheological polishing were investigated. On small-scale samples (22 mm and 6×6 mm), the target roughness ($R_q/\lambda < 0.012$) was achieved, while scaling to larger substrates revealed degradation of surface quality, indicating the need for further process optimization. The results confirm the applicability of the developed polishing techniques and provide a basis for a scalable preparation route for ITER optical components.

Keywords: abrasive polishing, magnetorheological polishing, steel 316L(N)-IG, ITER, second mirrors.

DOI: 10.61011/EOS.2025.08.62026.8165-25

Introduction

The optical system for radiation collection of the Thomson scattering diagnostic in the ITER divertor (DTS) includes a mirror system transmitting collected radiation outside the vacuum chamber and consists of the first mirror unit (First Mirror Unit, FMU) and 4 sequentially reflecting large-size mirrors („second mirrors“) [1], which are not exposed to contamination, and the key requirement for them is the maximum reflectance ($> 92\,\%$) in the range $540-1100$ nm and its stability under temperature fluctuations and possible water ingress into the vacuum volume. For the FMU, located in the area of intense thermal and radiation exposure, high thermal conductivity λ_{th} is important, so stainless steel 316L(N)-IG is not used, yielding to materials such as Mo, W, and CuCrZr [2,3] (table). Meanwhile, for the „second mirrors“, which are not subject to contamination and are mounted on a massive stainless steel structure [4], this material remains preferable due to its high thermal stability (E/ρ), shape stability, and structural compatibility with the support frame.

Austenitic stainless steel, chosen as the main structural material for ITER because of its non-magnetic properties, is not a traditional optical material due to its high ductility, which complicates obtaining optical-quality surfaces by grinding/polishing. Moreover, steel has a low reflectance ($\sim 60\,\%$) in the visible range, which makes it necessary to form a highly reflective coating on its surface to achieve the required optical characteristics. The reflectance of a highly reflective thin-film coating depends on the combined optical properties of the coating and the morphological characteristics of the substrate. Significant surface roughness increases diffuse scattering, and microscopic defects can create local stresses affecting the coating's durability. This necessitates achieving minimal subsurface defects, high cleanliness, and optimal microstructure for adhesion during polishing.

For quantitative assessment of scattering (Total Integrated Scattering, TIS) Bennett and Porteus [5] established a dependence on roughness:

$$\mathrm{TIS_{BP}} = R_0 \left[1 - e^{-\left(\frac{4\pi R_q \cos\theta_i}{\lambda}\right)^2}\right],$$

Mechanical properties of SS316L(N)-IG and other materials (at 20 °C)

	SS316L(N)	CuCrZr	W	Mo
Specific density γ (10^4 N m^{-3})	8.03	8.7	19.3	10.2
Modulus of elasticity E (GPa)	200	127.5	400	330
Specific stiffness E/γ (10^6m)	**2.5***	1.46	2.1	3.2
Thermal expansion coefficient α (10^{-6}K^{-1})	16	16.7	4.5	5.35
Thermal conductivity λ_{th} (W·m^{-1}K^{-1})	15	318	175	138
Temperature stability α/λ_{th} (10^{-8}mW^{-1})	**107****	0.5	2.57	3.9

Note: *Specific stiffness is comparable with other materials. **Best temperature stability, characterized by the ratio of the material's linear expansion coefficient to its thermal conductivity.

where R_0 is the theoretical value of surface reflectance, R_q is the root mean square surface roughness, θ_i is the angle of incidence on the surface, λ is the wavelength of light.

To ensure the operability of the ITER DTS radiation collection system, the key criterion is minimizing diffuse scattering expressed by the condition $TIS_{BP} < 1\,\%$. For steel 316L(N)-IG with a reflectance of$R_0 = 0.6$ ($\lambda = 540$ nm) this criterion is met at a root mean square roughness of $R_q < 6.4$ nm ($R_q/\lambda < 0.012$). However, achieving such parameters for stainless steel requires the development of specialized processing technologies. It should also be noted that the given criterion $R_q < 6.4$ nm is approximate, and its applicability in real conditions requires additional justification considering surface specifics and operational loads.

This work, without claiming a comprehensive solution, summarizes some experience in developing technological processes for abrasive and magnetorheological polishing of steel 316L(N)-IG. Abrasive processing of steel combines mechanical action of abrasive particles and chemical influence of surfactants [6]. The balance of these factors determines roughness, degree of subsurface damage, and electronic surface state. For example, reduction of the surface work function (electron work function, EWF) after abrasive processing reduces susceptibility to pitting corrosion [7], and adding oxidizer to the polishing suspension increases material removal rate and improves surface smoothness [8]. Abrasive grains act via two mechanisms: micro-cutting (constant surface contact) and micro-impact (periodic impact by loose grains) [9]. The first can cause scratches on the surface, while fine particles can penetrate the material (embedding) [10] forming a layer with unstable physico-mechanical properties [11,12]. Considering limited knowledge of the effect of the embedded layer on optical stability, its removal is mandatory. The principle of magnetorheological polishing (MRP) is based on changing the rheological properties of MRP fluid in a magnetic field [13,14]. In the treatment zone, a polishing zone forms: a solid-like core (elastic substrate) and a liquid layer with abrasives. Unlike traditional methods, MRP provides instant adaptation to the part surface without material damage and embedded layer formation [15]. However, MRPF processes are mostly developed for optical materials [16], unlike steels [17].

In this study, a comparative analysis of two approaches to forming an optically smooth surface on stainless steel 316L(N)-IG samples has been conducted. Surface topography parameters were obtained on optical profilometers Zygo ZeScope, 4D Technology NANOCAM, MicroXAM-800, as well as atomic force microscope INTEGRA-AURA. Sample surface morphology was studied using scanning electron microscope (SEM) MERLIN^{TM} in secondary electron detectors Everhart-Thornley (SE2), and elemental analysis was performed by energy-dispersive X-ray spectroscopy (EDX) on the INCA attachment. Diffuse scattering was measured on integrating sphere UPB-150-ART equipped with CAS140C-171 spectrometer. CAS140C-171.

Abrasive Polishing

Abrasive polishing technology aimed at minimizing the roughness parameter R_q was tested on model samples 22 mm diameter (Fig. 1, *a*). The processing was carried out on three groups of samples on a resin polisher using different suspensions based on diamond paste ASM 2/1, ASM 1/0 with $CuSO_4$ASM 0.5/0 with 2 % oxalic acid solution. The minimum root mean square roughness $R_q = 1.51$ nm was obtained using the fine fraction 0.5/0, while 2/1 gave the highest roughness$R_q = 2.31$ nm. Microscopic surface analysis after ASM 0.5/0 revealed two types of defects: randomly placed scratches and uniformly distributed carbon particles sized 50−200 nm (Fig. 1, *b*), not correlated with scratches, possibly indicating their embedding at an early stage of processing. The formed embedded layer has a depth of about 0.3 μm (Fig. 1, *c*), and the surface topography meets the required parameter $R_q/\lambda < 0.012$ (Fig. 1,*f*).

The scaling of the process was carried out on a large-sized M2 mirror 540 × 110 mm (Fig. 1, *d*). Studies of the polishing process revealed several key patterns and technological limitations. The main problem was the stable

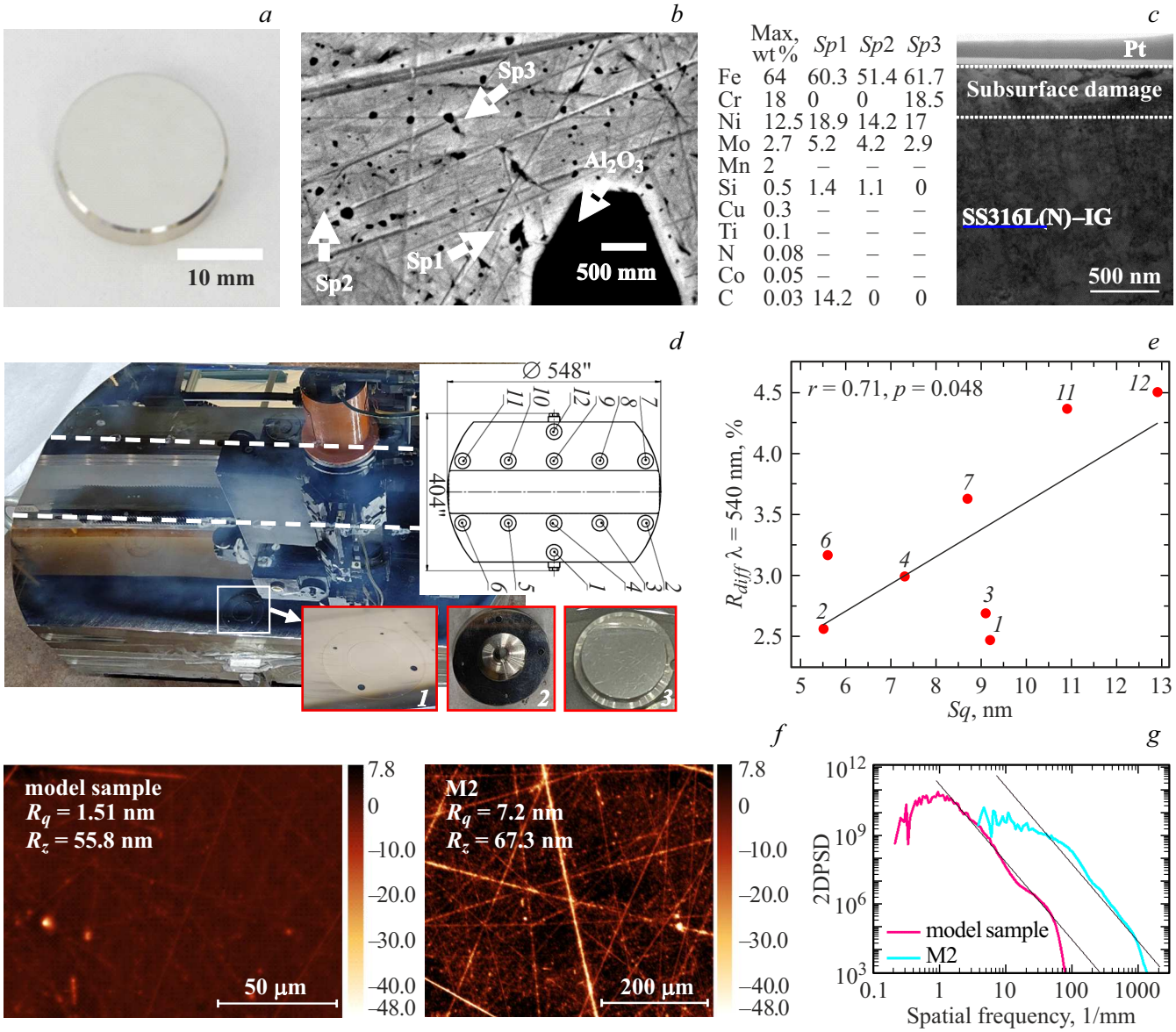

Figure 1. (*a*) Photograph of a model sample after polishing. (*b*) SEM+EDX-image at 50 K surface after polishing showing carbon inclusions. (*c*) TEM image of embedded layer after polishing. (*d*) Photograph of M2 mirror after polishing assembled with parasitic surfaces, into which witness samples are installed, where *1* witness sample assembly in parasitic surface holder, *2* holder of witness sample, *3* witness sample ∅22 mm. (*e*) Correlation between diffuse reflection and roughness parameter R_q of M2 mirror witness samples. (*f*) Surface topography of model sample and M2 mirror. (*g*) Comparison of 2D PSD function of model sample and M2 mirror surface.

alternation of two types of surface defects — pitting and lasing, and eliminating one defect type inevitably led to the appearance of the other. The polisher material showed significant influence on the result: resin polisher gave the best results in combination with suspensions based on aluminum oxide (WCA), while felt and polyurethane polishers were less effective and prone to cause pitting, especially when used with cerium oxide („U“ 0.8–1.2 μm, „D“ 0.4–0.6 μm, „Neva-3“). The most effective combination to combat pitting proved to be the use of a resin polisher with WCA-3 suspension (aluminum oxide, ∼ 3 μm) and the addition of glycerol, which ensured elimination of pitting after 8 hours of processing but caused the formation of numerous lasing defects. Diamond suspensions provide the best reflectivity and the lowest roughness, but do not eliminate pitting even after prolonged (60 hours) treatment.

The complexity of processing a large-sized part is associated with several factors: 1) increased abrasive lifetime, leading to changes in the dynamics of abrasive particle impact, 2) part of the surface is exposed and subjected to environmental effects, causing oxidation or other undesirable changes in the material structure.

For surface characterization (roughness and diffuse scattering), witness samples №1–12 ∅22 mm, located on

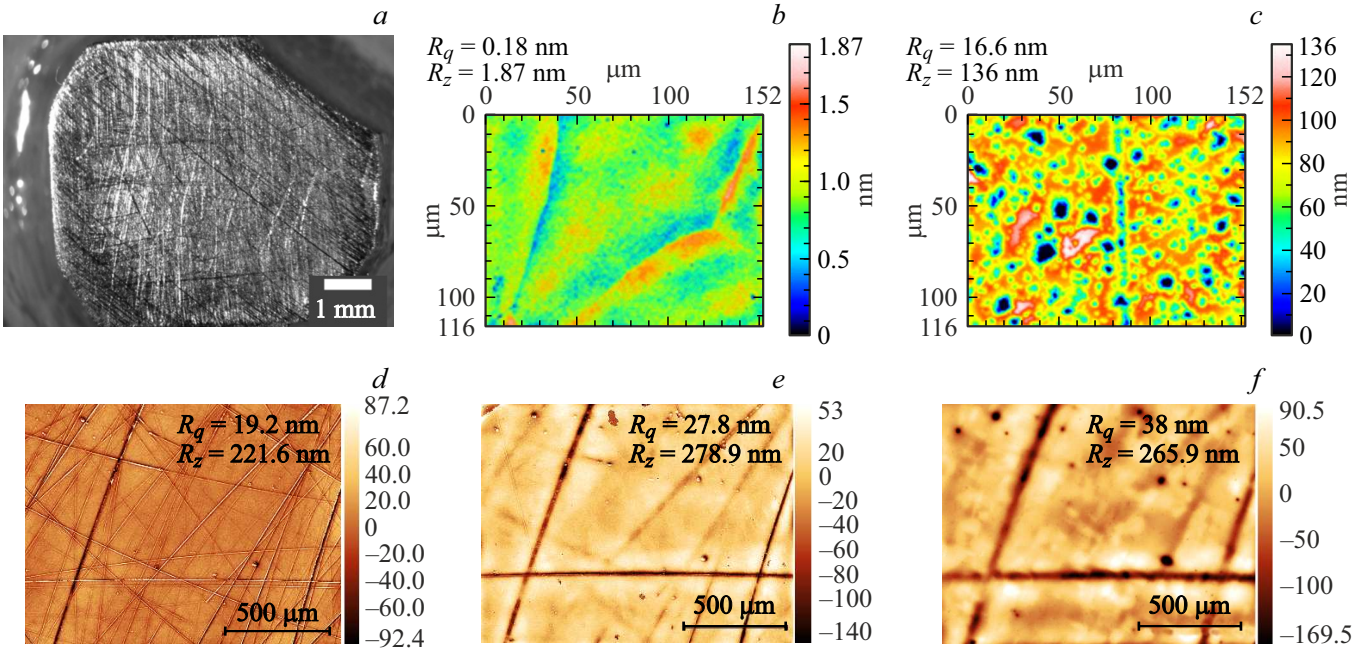

Figure 2. (*a*) Photograph of model sample 6 × 6 mm for testing various MRP fluid modes. (*b*) Surface topography of the model sample processed with MRP fluid composition № 5, (*c*) composition № 4. Processing on industrial equipment of witness sample № 10 of M2 mirror: (*d*) first treatment (∼ 100 nm), (*e*) second treatment (∼ 350 nm), (*f*) third treatment (∼ 800 nm).

parasitic surfaces of the M2 mirror block (Fig. 1, *d*, *1–3*) were extracted. The average value of R_q was 8.4 nm, about five times higher than the corresponding indicator for the model sample ($R_q/\lambda > 0.012$) indicating the need for technology optimization when scaling to large mirrors. A moderate positive correlation between roughness and diffuse reflectance $r = 0.71$, $p = 0.048$ (Fig. 1, *e*) was identified, confirming the influence of microgeometry on optical properties. The wavelength 540 nm was chosen as the most sensitive to scattering in the working range 540–1100 nm. For the M2 mirror, the measured roughnessR_q was 7.2 nm ($R_q/\lambda > 0.012$), explained by the presence of deeper scratches (Fig. 1,*f*). Analysis of 2D PSD showed extrema at low frequencies caused by data limitations on large scales, as well as a spectral density excess (∼ 1000 1/mm) for M2 compared to the model sample over a wide frequency range (Fig. 1, *g*), correlating with increased roughness.

Magnetorheological Polishing

Magnetorheological polishing (MRP) was carried out on a model sample 6 × 6 mm made of steel 316L(N)-IG (Fig. 2, *a*) in the laboratory setup „Polymag“ allowing effective study of various polishing fluid compositions due to the required small volume (∼ 50 ml). The initial surface after abrasive treatment with P240 disk (grain size 50–63 μm) had pronounced multidirectional scratches 50–200 nm deep and roughness parameters $R_q = 63.3$ nm, $R_z = 335$ nm.

The influence of magnetorheological polishing fluid (MRPF) composition and processing modes (soft/hard) was studied experimentally. The polishing mode was determined by the gap between the cuvette and the sample: decreasing the gap (2 mm) increased material removal intensity due to the concentration of magnetic particles near the surface but also increased the risk of deep defects. The soft mode (gap ∼ 4 mm) provided gentler treatment.

During the study, the effect of the MRPF composition on the polishing quality of steel 316L(N)-IG was investigated. The best results were achieved with MRPF composition No. 5 based on fine iron powder ($R_q = 0.18$ nm) (Fig. 2, *b*); the surface was uniform with a pronounced polycrystalline structure without signs of embedding. The worst quality was obtained with MRPF composition No. 4 based on ethyleneglycol ($R_q = 16.6$ nm) (Fig. 2, *c*); multiple pitting and absence of grain structure indicated process instability due to particle agglomeration, unsuitable viscosity, or adverse chemical effects. The magnetorheological polishing method enables achieving the required criterion $R_q/\lambda < 0.012$ on the surface 5 × 5 mm of steel 316L(N)-IG without forming a damaged layer. Scaling up involves transition to a 5-axis MRP machine with a completely different process kinematics, including relative motion scheme of tool and workpiece and supply of polishing suspension. Therefore, process parameters cannot be directly transferred to industrial setups.

Technology validation on industrial equipment was conducted on witness sample № 10 of the M2 mirror after abrasive polishing. The technological process consisted of three sequential processing cycles, resulting in removal of

a surface layer about 800 nm thick (Fig. 2, *d–f*). Gradual smoothing of the surface without formation of new defects was noted, though some deep scratches increased and roughness rose from $R_q = 19.2$ to $R_q = 38$ nm. The preserved metallic sheen indicated no signs of corrosion. The results confirm the potential of the method, but its scaling requires further optimization and research.

Conclusion

The study results highlight the need for precise control of polishing parameters when manufacturing mirrors for highly reflective optical systems. Typical defects, such as scratches, pitting, and oxide inclusions, can serve as model scenarios when evaluating the durability of mirror coatings under operational conditions.

Both studied technologies — abrasive and magnetorheological polishing — demonstrated the ability to achieve the required surface roughness $R_q/\lambda < 0.012$ on model samples made of stainless steel 316L(N)-IG. The best characteristics were obtained using MRPF composition No. 5 $R_q/\lambda < 0.0003$, with the surface structure distinguished by absence of embedding. The abrasive technology also showed high efficiency, providing target quality $R_q/\lambda < 0.003$. When scaling the process to a larger mirror, an increase in roughness was recorded, indicating the need for further optimization, including tool selection or modification of polishing regimes. Nevertheless, the demonstrated results confirm the applicability of the chosen approaches and create a solid foundation for advancing high-precision processing technology of large optics made of stainless steel 316L(N)-IG.

The article does not cover alternative approaches based on preliminary coating of the stainless steel surface with another material followed by processing — for example, diamond turning of bimetallic CuCrZr/SS316L(N)-IG construction or abrasive polishing of glassed steel surface SS316L(N)-IG. The choice of direct processing of the stainless steel substrate is driven by the desire for structural simplicity and technological reproducibility; however, evaluation of such combined solutions remains a subject for further research.

Funding

This work was partially supported by the Ministry of Science and Higher Education of the Russian Federation (agreement FFUG-2024-0034), and partially funded by the State contract No. H.4k.241.09.23.1060 within the ITER project. Microscopy was carried out at SPbU „Microscopy and Microanalysis“ Resource Center Microanalysis of coating samples was supported by Saint Petersburg State University (project code AAAA-A19119091190094-6).

Conflict of interest

The authors declare that they have no conflict of interest.

References

[1] D. Samsonov, I. Tereschenko, E. Mukhin, A. Gubal, Y. Kapustin, V. Filimonov, N. Babinov, A. Dmitriev, A. Nikolaev, I. Komarevtsev, A. Koval, A. Litvinov, G. Marchii, A. Razdobarin, L. Snigirev, S. Tolstyakov, G. Marinin, D. Terentev, A. Gorodetsky, R. Zalavutdinov, A. Markin, V. Bukhovets, I Arkhipushkin, A. Borisov, V. Khripunov, V. Mikhailovskii, V. Modestov, I. Kirienko, I. Buslakov, P. Chernakov, A. Mokeev, M. Kempenaars, P. Shigin, E. Drapiko. Nucl. Fusion, **62** (8), 086014 (2022). DOI: 10.1088/1741-4326/ac5368

[2] R. Santos, H. Policarpo, B. Goncalves, P. Varela, E. Nonbol, E. Klinkby, B. Lauritzen, Y. Romanets, R. Luis, P. Vaz. In: *Proc. of the 4th Int. Conf. on Advancements in Nuclear Instrumentation Measurement Methods and their Applications* (ANIMMA, 2015), p. 950. DOI: 10.13140/RG.2.1.5173.0001

[3] M. Joanny, S. Salasca, M. Dapena, B. Cantone, J. Travère, C. Thellier, J. Fermé, L. Marot, O. Buravand, G. Perrollaz, C. Zeile. Rev. Sci. Instrum., **83** (10), 10E506 (2012). DOI: 10.1063/1.4731004

[4] I. Kirienko, I. Buslakov, V. Modestov, I. Murtazin, E. Mukhin, A. Litvinov, A. Koval, D. Samsonov, V. Senichenkov, G. Marinin, D. Terentyev, P. Andrew. Fusion Eng. Des., **146**, 2624–2627 (2019). DOI: 10.1016/j.fusengdes.2019.04.058

[5] H. Bennett. Opt. Soc. Am., **51** (2), (1961). DOI: 10.1364/josa.51.000123

[6] A.P. Mitrofanov, K.A. Parsheva. Vestnik mashinostroeniya, bf 6, 75–79 (2017).

[7] A.P. Mitrofanov, K.A. Parsheva. Fizikohimiya poverhnosti i zashchita materialov, **56** (3), 330–336 (2020). (in Russian) DOI: 10.31857/S0044185620030249

[8] X. Hu, Z. Song, W. Liu, F. Qin, Z. Zhang, H. Wang. Appl. Surf. Sci., **258** (15), 5798–5802 (2012). DOI: 10.1016/j.apsusc.2012.02.100

[9] W. Liao, Y. Dai, Z. Liu, X. Xie, X. Nie, M. Xu. Opt. Express, **24** (4), 4247 (2016). DOI: 10.1364/OE.24.004247

[10] J. Yin, Q. Bai, B. Zhang, J. Chin. Mech. Eng., **31** (1), 41 (2018). DOI: 10.1186/s10033-018-0229-2

[11] A.V. Rogov, Yu.V. Kapustin, V.M. Gureev, A.G. Domantovskij. Poverkhnost: rentgenovskie, sinkhrotronnye i neytronnye issledovaniya **6**, (in Russian). 25–32 (2021). DOI: 10.31857/S1028096021060121

[12] A.E. Gorodetsky, A.V. Markin, V.L. Bukhovets, V.L. Voytitsky, T.V. Rybkina, R.Kh. Zalavutdinov, V.I. Zolotarevsky, A.P. Zakharov, I.A. Arkhipushkin, L.P. Kazansky, A.M. Dmitriev, A.G. Razdobarin, D.S. Samsonov, E.E. Mukhin J. Surf. Investig. X-Ray Synchrotron Neutron Tech., **14** (5), 1003–1015 (2020). DOI: 10.1134/S1027451020050298

[13] A. Hudolej. Nauka i innovacii, **11** (189), 31–39 (2018).

[14] A. Sidpara, M. Das, V. Jain. Mater. Manuf. Process., **24** (12), 1467–1478 (2009). DOI: 10.1080/10426910903367410

[15] M. Kumar, H. Singh Yadav, A. Kumar, M. Das. Micromanufacturing, **5** (2), 82–100 (2022). DOI: 10.1177/25165984211008173

[16] M. Tricard, W. Kordonski, A. Shorey, C. Evans. CIRP Ann., **55** (1), 309–312 (2006). DOI: 10.1016/S0007-8506(07)60423-5

[17] N. She, T. Gong, B. Chen, M. Lu, Y. Xu, X. Peng. Mech. Sci., **14** (1), 179–191 (2023). DOI: 10.5194/ms-14-179-2023

Translated by J.Savelyeva